CHALMERS
UNIVERSITY OF TECHNOLOGY

STRUCTURAL DYNAMICS OF A WIND TURBINE DRIVE TRAIN HIGH SPEED SUBSYSTEM: MATHEMATICAL MODELLING AND

Proceedings of ICoEV 2015 International Conference on Engineering Vibration

Ljubljana, 7 - 10. September

CIP
National and University Library of Slovenia

621.8.034(082)(0.034.2)

INTERNATIONAL Conference on Engineering Vibration (2015 ; Ljubljana)
Book of abstracts of ICoEV 2015 [Electronic source] / International Conference on Engineering Vibration, Ljubljana, 7 - 10. September ; [editors Miha Boltežar, Janko Slavič, Marian Wiercigroch]. - EBook. - Ljubljana : Faculty for Mechanical Engineering, 2015

ISBN 978-961-6536-97-4 (pdf)
1. Boltežar, Miha
281005824

11th International Conference on Engineering Vibration
Ljubljana, Slovenia, 7–10 September 2015

STRUCTURAL DYNAMICS OF A WIND TURBINE DRIVE TRAIN HIGH SPEED SUBSYSTEM: MATHEMATICAL MODELLING AND VALIDATION

Saeed Asadi*, Viktor Berbyuk, Håkan Johansson

Department of Applied Mechanics
Chalmers University of Technology
SE-41296, Gothenburg, Sweden

{saeed.asadi,viktor.berbyuk,hakan.johansson}@chalmers.se

Keywords: Wind turbine drive train, High speed shaft subsystem, Torsional vibrations, Model validation, Motor model

Abstract. *The paper studies the dynamics of a wind turbine drive train high speed subsystem, both by modelling and experiments with focus on system torsional vibration and transient events which can reduce fatigue life of functional components (gearbox, bearings, shafts, couplings, others). A scaled down drive train high speed shaft test rig has been developed. Main components of the test rig are six-pole motor with variable frequency drive controller (up to 1000 rpm), shafts' disk coupling and flexible mounting structure representing gearbox housing with output high speed bearing. The test rig is equipped with measurement system comprising a set of accelerometers and displacement sensors, strain gauges and telemeter system, data acquisition hardware and software (SKF WindCon3.0). Mathematical and computational models of the test rig have been developed and went through validation tests. The system dynamic response is studied for different operational scenarios and structural parameters (run-shut down case with and without eccentric mass). The ultimate goal of the test rig is to get insight into interaction between internal dynamics of drive train mechanical and electrical functional components and to develop novel methods to detect, predict and prevent faults and failures in wind turbine drive trains arising due to misalignments and transient external loads.*

1 INTRODUCTION

Wind energy conversion systems are one of the fastest growing global source of new electric generation and it is estimated to remain so for some time. Since mechanical vibrations of wind turbine drive train system become coupled with the electrical vibrations of currents in the motor winding, therefore it is important to include electromechanical interaction between different components in wind turbine system modelling. This leads to improve reliability by better prediction of the risk for different kinds of faults arising due to electromechanical failures demanding for better understanding of motor behaviors. A comprehensive yet ever growing list of the researches dealing with diagnostic problem of electric machines are presented in [1, 2].

In order to model and predict these electromechanical faults in drive train, the motor must be modeled in a sufficiently enough detail yet simple to avoid the complexity [3]. In many cases, this simplifications yield sufficiently useful results, but since many qualitative dynamic properties of the mechanical systems (their mass distribution, torsional flexibility and damping effects) are being neglected, they can lead to inaccuracies.

In wind turbine industry, Special attention was directed to induction motor (and squirrel cage which is used for grid connection) because of known reason such as size, cost, efficiency [4]. Therefore it is expected to model this specific motor. The model must describe the torsional oscillation phenomenon occurring in a multiple winding induction machine. The simplified faults in the induction motors can be categorized as induction motor mechanical faults (bearing, gearbox, oscilation and eccentricity) and electrical faults such as rotor (broken rotor bar and end rings) and stator faults (windings and external faults) [5].
A Gomez-Espinosa and V.M. Hernandez-Guzman have presented a new self-tuning algorithm which is developed for determining the Fourier Series controller coefficients with the aim of reducing the torque ripple in a PMSM, thus allowing for a smoother operation [6].
To support ongoing research with the aim to better predict what kinds of loads and electromechanical interactions that arise in a wind turbine drive train, a scaled down test rig relevant to the high speed subsystem of an indirect drive wind turbine has been developed [7, 8].

In this contribution, the mechanical characteristics of the test rig focusing on the motor response and torsional vibration, are presented, and used to validate its mechanical model. A simplistic model for the induction 3 phase motor is proposed by considering slip and torque ripple causing the failures. After model validation, the influence of eccentric mass and run-shut down case both in different motor speeds and corresponding modal analysis is studied, and the paper ends with conclusion and outlook.

2 DRIVE TRAIN HIGH SPEED SUBSYSTEM TEST RIG

2.1 Mechanical setup and instrumentation

To investigate wind turbine drive train system dynamics, a scaled down test rig has been built and instrumented. It entails a motor, rotor disk with shaft, where the rotor shaft is passing through the bearing housing and connected to the motor by a coupling. A small eccentric mass can be added on the rotor disk to give a uneven inertia distribution and in this way introduce to

the rotor system varying dynamic load. The setup of the drive train high speed subsystem test rig is depicted in Fig. 1.

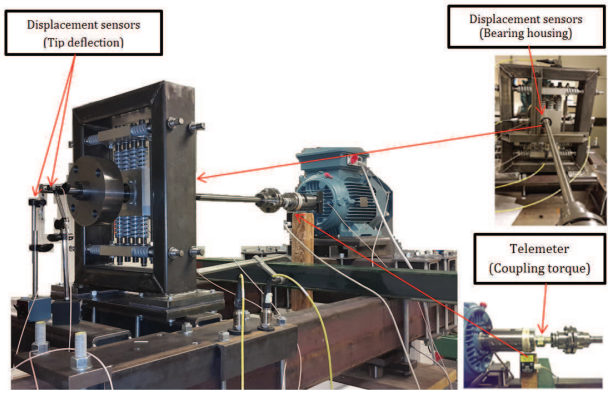

Figure 1: The test rig and its main components with sensors location

The main components of the test rig are ABB motor model M3BP160 MLA 6 (6 pole, 75 kW), with a frequency converter that controls motor speed up to 1000 rpm, motor shaft adapter, shaft's coupling, bearing housing with flexible support, a disk on which an eccentric mass can be added, bedplate on which all the components are mounted. The data acquisition has been done by SKF @ptitude Observer, that SKF offers under its WindCon3.0 condition monitoring system. The set of sensors comprise accelerometers (CMSS 7799 LF, CMSS 2200), and 4 Eddy probes displacement sensors (CMSS 665), which are used to assess vibrations in the test rig and deflection at both shafts tip and bearing housing. Additionally, in order to measure the torque in coupling, full bridge strain gauges are put on the motor shaft, and the signal is acquired using a telemeter system (TEL 1-PCM). Detailed specification of the sensors and their location are presented in Tab. 1.

Table 1 Sensors specifications and locations

Sensor name	Sensitivity	Range	Location
CMSS 7799 LF	500 mV/g	10 g peaks	Bearing housing
CMSS 2200	100 mV/g	80 g peaks	Bearing housing
CMSS 665	7.87 mV/μ m	[0.2, 2.3] mm	Bearing housing and tip
Strain gauge (full bridge) with TEL 1-PCM	0.065 mV/Nm	50 V	Coupling
ABB motor model M3BP160 MLA 6			

2.2 Test rig characterization

2.2.1 Torque ripple in the motor

When running the motor frequency converter with 0 Hz frequency, there are some vibrations which can be seen in the motor, 50 Hz frequency appears in the frequency domain which reveals the existence of torque ripple in the motor torque (see Fig. 2).

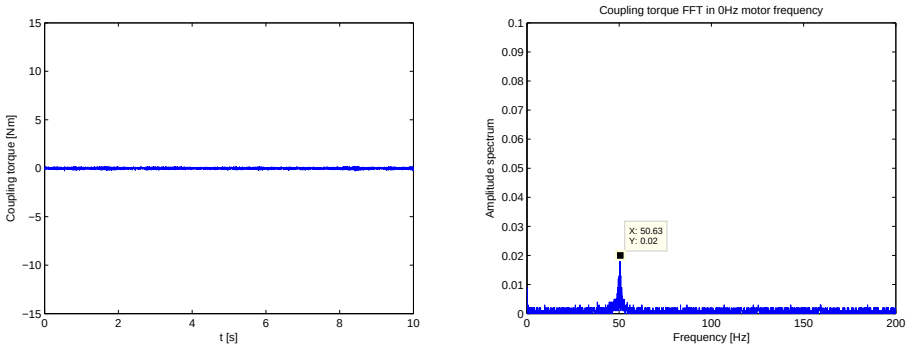

Figure 2: Coupling torsional torque, converter on with 0 Hz frequency (no running) (left) and corresponding FFT (right)

2.2.2 Knock test

In order to investigate the torsional eigenfrequency of the structure, knock test has been performed as shown in Fig. 3.

- A single pronounced peak around 49.5 Hz was seen in frequency diagram which refers to the fundamental torsional eigenmode (6 repetitions gave $f = [49.438, 49.406, 49.406, 49.531, 49.281, 49.344]$ Hz). Since the motor adds substantial damping to the system, it is expected that a measured vibration will be at a somewhat lower frequency (in subsequent analyses a peak at 48.5 Hz was often seen during running).
- In the amplitude spectrum, a small peak at 50 Hz was also seen which seems to be due to a leaking current or some other electrical interference from grid.

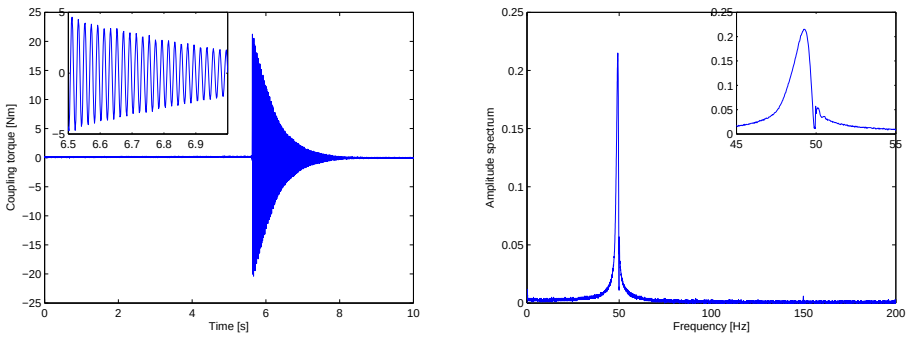

Figure 3: Coupling torsional torque in the knock test (left) and corresponding FFT (right)

2.2.3 Direct connection to the grid

In order to understand the effects of the motor converter to the response of the system, a test is run when motor is fed by direct connection to the grid (50 Hz) circumventing the converter.

Here is the results which are different compared to previous case.

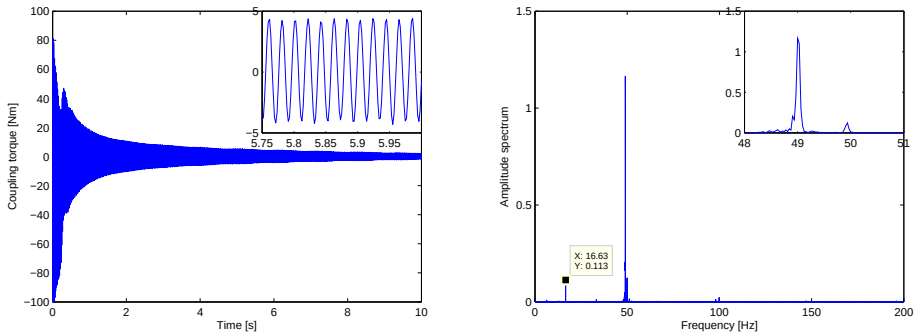

Figure 4: Coupling torsional torque in direct connection to grid, 50 Hz (left) and corresponding FFT (right)

The peaks in the frequency domain, correspond to motor mechanical (16.63 Hz) and electrical (50 Hz) frequencies since the motor is 3 phase. Also since the motor is directly supplied from the grid, we do not see any torque ripple in the steady state regime.

3 TORSIONAL VIBRATION MODEL OF DRIVE TRAIN TEST RIG

An engineering model and the sketch of the test rig are shown in Fig. 1 and Fig. 6 respectively. The mechanical model has been developed based on both rigid and flexible shaft assumption in bending modes, considering that the torsional flexibility is concentrated at coupling. The shaft twist is represented by $\Delta \stackrel{def}{=} \phi_g - \phi_r$, where $\phi_r(t)$ and $\phi_g(t)$ correspond to the rotor and motor shafts' angles, respectively. The motor is rigidly attached to the bedplate, the bearing housing flexibility is assumed linear.
In order to have a better insight into different operation points, Campbell diagram is shown in Fig. 5. Here, the torsional frequency and bending frequency related to the first bending eigenmode [9], the operating motor speed and 3X motor speed have been illustrated. Results below are considered motor speeds 600, 800, 1000 rpm, indicated as vertical lines.

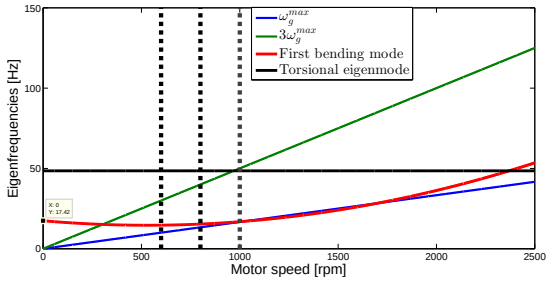

Figure 5: Campbell diagram

It could be perceived that since the second bending eigenmode is higher than the relevant

excitation frequency, it is sufficient to define the deflection field based on the first bending eigenmode (17.42 Hz). Furthermore, a motor speed of 1000 rpm is close to a critical speed.

A model for shaft bending and twist was developed in [10] where it was found that a torsional and deflection fields do not affect significantly and for studying of the torsional response of the test rig, assuming the pure torsional model is sufficient [10].

Here, we shall focus on a lumped torsion vibration model for the drive train test rig. An engineering abstract of the model is depicted in Fig. 6 and entails two inertias, disk J_r and generator rotor J_g, respectively. Each of these inertias are supported by bearings, whose internal friction is represented by torsion dashpots. The shaft and coupling flexibility is lumped together and represented by a torsion spring. Due to gravity and eccentric mass, there will be an external torque $M_r(= m_e r_e g \cos\phi_r)$ acting on the disk, and the induced electrical torque from the motor M_g acts on the generator rotor.

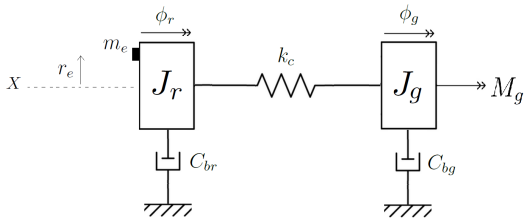

Figure 6: Engineering abstract of the test rig in torsional vibration

Hence, we have the following set of equations to describe the test rig torsional vibration response:

$$J_r\ddot{\phi}_r + C_{br}\dot{\phi}_r + k_c(\phi_r - \phi_g) = -m_e r_e g\cos\phi_r \tag{1}$$

$$J_g\ddot{\phi}_g + C_{bg}\dot{\phi}_g + k_c(\phi_g - \phi_r) = M_g(t) \tag{2}$$

The motor is a 6 pole induction machine with rated power 7.5 kW at speed 975 rpm. The speed is set from a frequency converter, such that the torque is given by the difference from set speed ω_g^{set} and actual speed $\dot{\phi}_g$. A cycle of ramp startup - steady state - shut down can thus be described by:

$$M_{\text{mech}} = \frac{M_{\text{mark}}}{\Delta\omega_{\text{mark}}}\left(\omega_g^{set} - \dot{\phi}_g\right) \quad \text{where} \begin{cases} \omega_g^{set} = \frac{t}{t_0}\omega_g^{max} & t < t_0 \\ \omega_g^{set} = \omega_g^{max} & t_0 \le t < t_1 \\ M_{\text{mark}} = 0 & t_1 \le t \end{cases} \tag{3}$$

where $\Delta\omega_{\text{mark}} = 25/60 \times 2\pi$ rad/s, $M_{\text{mark}} = 73.4561$ Nm, t_0 is the startup-time, and t_1 is the instance when motor is turned off (without braking). From electrical measurement of the voltage from the frequency converter, it was found that in addition to M_{mech}, there is a small periodic torque (ripple) acting on the generator rotor with at frequencies ω_g^{set}, $3\omega_g^{set}$ and $6\omega_g^{set}$. Hence, the following electrical torque is considered

$$M_g(t) = \frac{M_{\text{mark}}}{\Delta\omega_{\text{mark}}}\left(\omega_g^{set} - \dot{\phi}_g\right) + M_{rip1}\sin(\phi_g) + M_{rip2}\sin(3\phi_g) + M_{rip3}\sin(6\phi_g) \tag{4}$$

where $M_{rip1,2,3}$ ($= 10$ Nm) are coefficients that contribute to torque ripple with corresponding frequencies and have been obtained based on comparison of the torque ripple range in steady state in simulation and experiments.

The parameters and their numerical values used in the model are given in Tab. 2.

Table 2 Test rig numerical parameters

Parameter	Symbol	Value
Rotor inertia with respect to ϕ_r	J_r	J_r = 0.095 kgm^2
Rotor inertia	J_g	J_g = 0.087 kgm^2
Coupling torsional stiffness	k_c	$k_c = 2600$ N/rad
Rotor torsional damping coefficient	C_{br}	$C_{br} = 0.006$ N/m
Motor torsional damping coefficient	C_{bg}	$C_{bg} = 0.006$ N/m
Eccentric mass mounted in the rotor disk	m_e	$m_e = 74.4$ gr
Distance of eccentric mass from center	r_e	$r_e = 8$ cm

4 EXPERIMENTAL AND SIMULATION RESULTS

The torsional vibrations of the system in both experiment and simulation have been analyzed and qualitatively validate the mechanical model for torsional response in time and frequency domains.
The coupling torque in the mechanical model is computed as: $M_\Delta(\Delta(t)) = k_c \times \Delta$. The following plots show the coupling torsional torque representing the torsional dynamic response of the system.

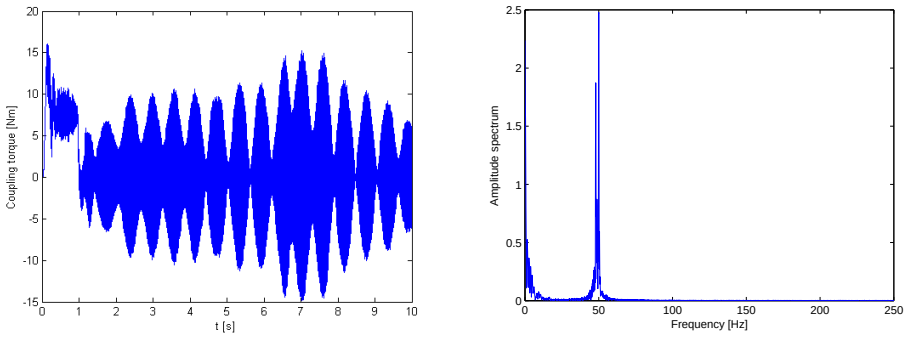

Figure 7: Coupling torsional torque (with frequncy converter) in experiment in 50 Hz (left) and corresponding FFT (right)

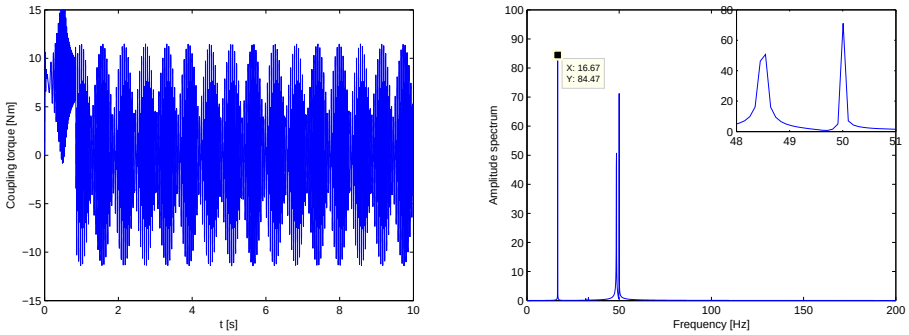

Figure 8: Coupling torsional torque in simulation in 50 Hz (left) and corresponding FFT (right)

As demonstrated by Fig. 7 and Fig. 8, the responses of the system in both simulation and experimental test data in terms of coupling torque are quite similar with respect to amplitude and frequency in steady state phase, but not so much similar in transient phase. The experimental results on coupling torque show a strong modulated oscillation, which seems to be due to motor excitation close to torsional eigenmode, as in the mechanical model it has been modeled as motor torque ripple.
As part of the model validation, the steady state responses of the system from experiment and simulation, with respect to different motor speeds are in Fig. 9.

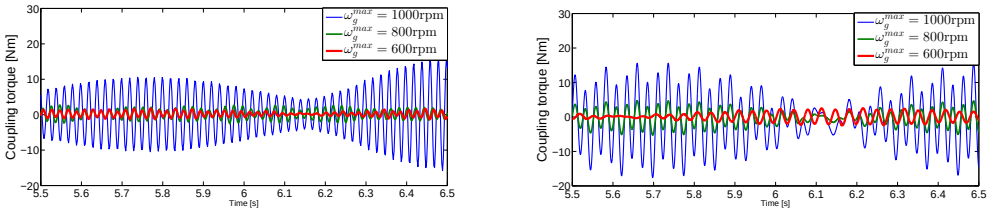

Figure 9: Coupling torsional torque in steady state regime experiment (left) and simulation (right) wrt different motor frequencies

As interpreted from Fig. 9, in the simulation results, the coupling torque range is smoothly decreasing by smaller motor frequency, whereby this decrease in the experiment is significant. This might be due to the nonlinear dependency of the ripple coefficients in the Eqn. 4 ($M_{rip1,2,3}$).

The following graphs show the load cycle defined in Eq. 3 in both simulation and experiment with and without eccentric mass, in different motor speeds. It must be noted that in the experiment, the minor fluctuations in the starting time of data acquisitions and shut down time are due to that they are manually imposed. Also in the simulation, the steady state time span runs for 10 seconds (in $[1, 11]$ sec).

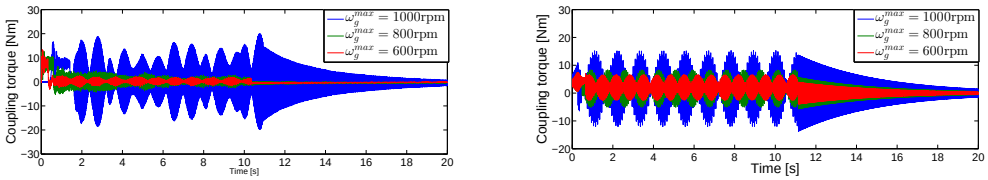

Figure 10: Coupling torsional torque in run-shut down in experiment (left) and simulation (right)

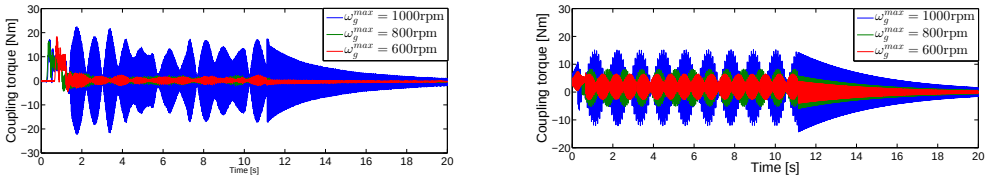

Figure 11: Coupling torsional torque in run-shut down in experiment (left) and simulation (right) with no eccentric mass ($m_e = 0$)

As demonstrated from Fig. 10 and Fig. 11, the simulation response in run-shut down case is quite similar to the experiment, specially in steady state and shut down regime. Also, an experiment without any eccentric mass was conducted. Now, consider the eccentric mass effect as a external torque. Comparing eccentric case and no eccentric case, the range of coupling torque when the eccentric mass is applied, is increased since there is more external torque applied to the system.

5 CONCLUSION AND OUTLOOK

The test rig has been developed to study the dynamics of high speed shaft subsystem of wind turbine drive train. The mathematical and computational models of the test rig have been developed by taking into account torsional flexibility of shafts and coupling and qualitatively validated. The simulation results have been represented based on different operational scenarios (different motor speed, run-shut down case). The results allow one to analyze a dynamic response of a misaligned shaft and coupling as well as reactions that affect bearing.
The proposition for the future works could be outlined as follows:

1. Define more realistic ripple coefficients contributing the specific frequencies in torque ripple.
2. Employ the Park model [2] to better describe the induction motor, where the development of its current, torque and power relationships are based on the assumptions that the rotating magneto motive force produced by stator winding excitation is sinusoidally distributed in space and that the rotor mmf due to the slip frequency induced currents is similarly distributed. The stator currents should in this case be given correspondiong to the pertinent frequency controller output.

Acknowledgment This project is financed through the Swedish Wind Power Technology Centre (SWPTC). SWPTC is a research centre for design of wind turbines. The purpose of the centre is to support Swedish industry with knowledge of design techniques as well as maintenance in the field of wind power. The Centre is funded by the Swedish Energy Agency, Chalmers University of Technology as well as academic and industrial partners. In particular,

donations of motors and frequency converters by ABB CR, WindCon3.0 condition monitoring system and set of sensors by SKF are gratefully acknowledged. Besides, the authors would like to thank Jan M´oller for his contribution in the laboratory.

REFERENCES

[1] M. Benbouzid, Bibliography on induction motors faults detection and diagnosis, IEEE Trans. on Energy Conversion, vol. 14, no. 4, pp. 10651074, 1999. [Online]. Available: http://dx.doi.org/ 10.1109/60.815029

[2] T. Lindh, On the Condition Monitoring of Induction Machines. Lappeenranta: Lappeenranta University of Technology, 2003.

[3] T. Szolc, R. Konowrocki, M. Michajlow, A. Pregowska, An investigation of dynamic electromechanical coupling effect in machine drive systems driven by asynchronous motors, Mechanical systems and signal processing, 4(2), pp.118-134, 2014

[4] R. You, B. Barahona, J. Chai, N. A Cutululis, A Novel Wind Turbine Concept Based on an Electromagnetic Coupler and the Study of Its Fault Ride-through Capability, 11/2013; 6(11):6120-6136. DOI: 10.3390/en6116120

[5] K.S. Gaeid, H. Wooi Ping, M. Khalid, A. Lauy Salih, Fault Diagnosis of Induction Motor Using MCSA and FFT, Electrical and electronic engineering. 1(2), pp.85-92 2011. DOI: 10.5923/jeee.20110102.14.

[6] A. Gomez-Espinosa, V. M. Hernandez-Guzman, M. Bandala-Sanchez, A New Adaptive Self-Tuning Fourier Coefficients Algorithm for Periodic Torque Ripple Minimization in Permanent Magnet Synchronous Motors (PMSM), International Journal of advanced manufacturing technology, 2013, 13(3), 3831-3847; doi:10.3390/s130303831.

[7] McCainn, S.G., 2013:30, Design of Experiments and Analysis for Drive Train Test Rig, Masters Thesis, Department of Applied Mechanics, Chalmers University of Technology, Goteborg, Sweden

[8] Squires, J.C., 2014:36, Measurement System Design and Experimental Study of Drive Train Test Rig, Masters Thesis, Department of Applied Mechanics, Chalmers University of Technology, Goteborg, Sweden

[9] Silva, T., Maia, N., 2011, Elastically restrained Euler-Bernoulli beams applied to rotary machinery modelling, Acta Mech Sin, 27(1), pp. 5662.

[10] Asadi. S, Berbyuk. V, Johansson. H, 2015:30, Vibration Dynamics of a Wind Turbine Drive Train High Speed Subsystem: Modelling and Validation, ASME 2015 International Design Engineering Technical Conferences Computers and Information in Engineering Conference. 2015: August 2-5, 2015, Boston, Massachusetts, USA, paper DETC2015-46016.